Symbol Lock Detection in the ARX II and Block V Receivers

M. Shihabi and S. Hinedi
Communications Systems Research Section

B. Shah
Radio Frequency and Microwave Subsystems Section

The performances of five symbol-lock detectors are compared in this article. These detectors are the square-law detector with overlapping (SQOD) and nonoverlapping integrators, the absolute-value detectors with overlapping and nonoverlapping integrators, and the signal-power estimator detector (SPED). The analysis considers various scenarios in which the observation interval is much larger than or equal to the symbol-synchronizer loop bandwidth, and which have not been considered in previous analyses. Also, the case of threshold setting in the absence of signal is considered.

It is shown that the SQOD outperforms all others when the threshold is set in the presence of a signal, independent of the relationship between loop bandwidth and observation period. On the other hand, the SPED outperforms all others when the threshold is set in the presence of noise only.

I. Introduction

The Advanced Receiver II (ARX II) and Block V Receiver currently under development [1] use phase-locked loops (PLL's) to track the carrier, subcarrier, and symbol phase. Like most coherent receivers, the ARX II and Block V rely on lock detectors to provide the lock status of its PLL's. Since carrier, subcarrier, and symbol synchronization need to be achieved before any "meaningful" symbol detection can be initiated, lock detectors play a vital role in the final decision of accepting or rejecting the detected symbols. During operation, a loop is assumed to be locked when its lock indicator consistently has a positive status. The carrier and subcarrier lock detectors used in the ARX II and Block V Receiver have already been analyzed [2,3]. This article analyzes five candidate symbol-lock detectors for these receivers.

The detectors considered in this article are divided into two groups. The detectors in the first group process the outputs of two overlapping integrators, whereas those in the second group use two contiguous outputs of a single integrator. The first class contains two well-known lock detectors that use either squaring or absolute-value operations on the integrator outputs. The second class consists of three lock detectors, two of which use the same mathematical operations as those in the first class, while

the third detector functions as a signal power estimator. The five schemes are compared based on the lock-detection probability as a function of the symbol SNR for a given false-alarm probability and a fixed observation interval.

Although symbol-lock detection has been addressed before [4,5], the analyses have neglected the interdependence between symbol synchronizer bandwidth and lock detector bandwidth. The symbol synchronizer bandwidth refers to the one-sided loop noise bandwidth B_L of the digital data-transition tracking loop [6] used in the ARX II and Block V. The lock detector bandwidth is defined as the frequency at which the lock detector provides a status, being in- or out-of-lock. For example, the lock detectors considered here indicate loop status once every M symbols. Consequently, the bandwidth of these detectors is $1/(MT)$, where T is the symbol duration. The probability of false alarm P_{fa} is defined in two ways. In the classical sense, it is defined as the probability of declaring a signal (or target, as in radar applications) to be present when it is not present. In deep space applications, however, it is more appropriate to define P_{fa} as the probability of declaring a loop to be in-lock when it is out-of-lock. That is, P_{fa} is the probability of declaring the timing error to be "zero" (in-lock) when the loop is slipping cycles and operating with a nonzero timing error (out-of-lock).

In Section IV, the false alarm rate is shown to be drastically different, depending on the definition used. In addition, when the loop is slipping cycles, the false alarm rate is shown to depend strongly on the ratio of the lock detector bandwidth to the symbol loop bandwidth. For example, when the loop is slipping and $1/B_L \ll MT$, the lock detectors operate with acceptable false alarm rates because there are several uncorrelated samples of the timing error τ within the MT-sec decision interval. On the other hand, when $1/B_L \gg MT$, the false alarm rates are unacceptable because the timing error is constant over several decision intervals (see Section IV). Note that a good rule of thumb is to assume that the loop provides uncorrelated phase estimates every $1/B_L$ sec. As a result, the symbol timing error at time t_i is uncorrelated with the symbol timing error at time t_j, when $|t_i - t_j| \geq 1/B_L$. This article considers the special cases of $1/B_L = MT$ and $1/B_L = T$. The first case is analyzed and simulated, whereas the second case is simulated, but not analyzed. When the threshold is adjusted in the presence of noise only, the performance can be derived from the previous analysis by setting the signal amplitude to zero.

The description of the various lock detectors is presented in Section II. The general analysis and summary of the theoretical results are presented in Section III. The discussion of the theoretical, as well as the simulated, results is carried out in Section IV, followed by the conclusion in Section V. In Appendices A through F, some of the mathematical details are provided.

II. Description of the Lock Detectors

Figure 1 is a block diagram showing the signal processing functions common to the lock detectors surveyed in this article. The received signal is assumed to have been mixed with perfect carrier and subcarrier references so that the input to the lock detectors is a baseband signal of the form

$$r(t) = Ad(t) + n(t) \tag{1}$$

where A is the signal amplitude and A^2 is the received data power with

$$d(t) = \sum_{k=-\infty}^{\infty} d_k p(t - kT) \tag{2}$$

and where $n(t)$ is the additive white Gaussian noise process with a single-sided power spectral density (PSD) N_0 (watt/Hz). The data symbol d_k takes on the value ± 1 equally likely, and $p(t)$ is the received pulse shape of duration T sec. For comparison purposes, only the nonreturn-to-zero pulse is considered in the analysis, but the results can be extended to any pulse shape. The receiver is assumed to have perfect knowledge of T, but not the symbol epoch—i.e., the receiver has perfectly estimated the symbol rate, but not necessarily the start and end of the symbols.

The signal processing functions for the "lock detector" block in Fig. 1 depend on the detector being implemented. Its output X_k is at the symbol rate and, typically, many samples of X_k are averaged to obtain the decision statistic Y. If Y is greater than the threshold δ, the loop is declared to be in-lock, otherwise it is declared to be out-of-lock.

The parameter τ in Fig. 1 is the phase error between the symbol phase and the phase estimate provided by the symbol synchronizer. The in-lock case is analyzed by setting the timing error τ to zero. In practice, the error is not identically zero, but it is a very small value. When there is a signal present, the out-of-lock model for τ depends on the relation between B_L and $1/(MT)$. When $B_L = 1/(MT)$, τ is modelled as an unknown constant over a decision interval (MT sec), but one that is independent and uniformly

distributed from one decision interval to the next. Alternatively, when $B_L = 1/T$, the timing error is modelled as a constant over a symbol interval (T sec), but one that is independent and uniformly distributed from symbol to symbol. In this case, if the decision time $MT \gg T$ (as it usually is), each decision statistic encompasses the entire range of τ. When there is no signal present, the model of τ is irrelevant because the out-of-lock performance is independent of τ.

The detectors considered in this article are the square-law detector with overlapping (SQOD) and nonoverlapping (SQNOD) integrators, the absolute-value detectors with overlapping (AVOD) and nonoverlapping (AVNOD) integrators, and the signal-power estimator detector (SPED). The SQOD is depicted in Fig. 2(a). The input signal $r(t)$ is integrated over two symbol periods: one inphase with the estimated symbol interval and the other staggered by half a symbol duration. The resulting inphase and quadraphase samples I_k and Q_k are correlated due to the overlapping intervals. The AVOD detector replaces the squaring operations in Fig. 2(a) with absolute-value operations. Hence, its I and Q samples are also correlated. The SQNOD detector processes two contiguous outputs of a single integrator, as shown in Fig. 2(b). As before, replacing the squaring operations with absolute values yields the detector's counterpart, the AVNOD. The integrator outputs in this case are uncorrelated because the intervals are disjointed. The SPED detector is shown in Fig. 2(c). The SPED detector is considered because it is already part of the split-symbol moments' symbol-to-noise-ratio (SNR) estimator [7], the SNR estimator used in the ARX II and Block V. The inphase and quadraphase outputs of the SPED are obtained, respectively, by integrating the received signal over the first and second halves of a symbol. Since the noise in the first and second halves are independent, taking the product of I and Q and averaging over many symbols provides an estimate proportional to signal power.

III. Performance Analysis

The in-lock and out-of-lock performances of the lock detectors are derived in this section. The in-lock performance is measured in terms of the probability of declaring the loop to be locked when there is no timing error—that is, the probability that the decision statistic Y in Fig. 1 is greater than the threshold δ when $\tau = 0$. Note that $\tau = 0$ or no phase-tracking error is equivalent to setting the symbol synchronizer loop SNR to infinity. The degradation in detection probability due to timing jitter (a noninfinite loop SNR) is minimal and has been addressed in the case of carrier lock detectors [2]. The out-of-lock performance is measured by the probability of false alarm—the probability of declaring the loop to be locked when it is not locked. The out-of-lock performance in the presence of a signal is analyzed for the case $B_L = 1/(MT)$. The simulation results for $B_L = 1/T$ are presented in the next section.

Note that when $B_L = 1/T$, the timing error is independent from one symbol to the other, and the decision is made after averaging many, say M, symbols. On the other hand, when $B_L = 1/(MT)$, τ is an unknown constant during a decision interval, and is independent from one decision to the next. Setting $M = 1$ in the latter case would imply a decision for every symbol, which is fundamentally different from the case where $B_L = 1/T$ and the decision is made by using M symbols. Hence, the performance when $B_L = 1/T$ cannot be derived from the case of $B_L = 1/(MT)$ simply by setting $M = 1$. The out-of-lock performance when there is no signal present is also analyzed. Only the final equations are shown with the derivations detailed in the various appendices. In all cases, the decision statistic can be expressed as

$$Y = \frac{1}{M}\sum_{k=1}^{M} X_k \tag{3}$$

where the random variable X_k is peculiar to each detector. When the timing offset $\tau = 0$, the adjacent samples X_k and X_{k+1} are correlated in the first two detectors. Whereas for the remaining three detectors, they are uncorrelated. In all cases, the random variable X_k is not Gaussian due to the nonlinear operations on I_k and Q_k. For large values of M, the random variable Y is modelled as Gaussian due to the central limit theorem (CLT). The theorem applies to the sum of correlated random variables when none of the variables being summed dominates over the others [8]. This model for Y is justified by simulation results.

The probability of lock detection is the probability that the Gaussian random variable Y surpasses the threshold δ. Hence, it is given by

$$P_D = \int_{\delta}^{\infty} \frac{1}{\sqrt{2\pi\sigma_Y^2}} \exp\left[-\frac{(y-\mu_Y)^2}{2\sigma_Y^2}\right] dy \tag{4}$$

where μ_Y and σ_Y^2 are the mean and variance of Y when τ is exactly zero. By using the definition of the error function

$$\mathrm{erf}(x) \triangleq \frac{2}{\sqrt{\pi}} \int_0^x \exp(-t^2)dt \tag{5}$$

one has

$$P_D = \frac{1}{2} - \frac{1}{2}\,\mathrm{erf}\left(\frac{\delta - \mu_Y}{\sqrt{2}\sigma_Y}\right) \tag{6}$$

or

$$P_D = \frac{1}{2} - \frac{1}{2}\,\mathrm{erf}\left(\frac{\delta}{\sqrt{2}\sigma_Y}\sqrt{\frac{SNR_D}{2}}\right) \tag{7}$$

where SNR_D denotes the detector SNR defined by

$$SNR_D \triangleq \left(\frac{\mu_Y}{\sigma_Y}\right)^2 \tag{8}$$

The threshold δ is chosen to maintain a fixed probability of false alarm. The probability of false alarm is the probability that the out-of-lock decision statistics do not surpass the threshold. Hence, it is given by

$$P_{fa} = \int_{-\infty}^{\delta} f_o(y)dy \tag{9}$$

where $f_o(y)$ is the out-of-lock density of Y. The threshold δ is computed by solving Eq. (9) for a fixed P_{fa}. When there is a signal present and $B_L = 1/(MT)$, the statistic Y is no longer Gaussian and $f_o(y)$ must be obtained numerically or by simulation, as shown in Section IV. When there is no signal present, the CLT can be invoked and the out-of-lock decision statistic can be modelled as Gaussian. This model is verified by simulations in Section IV. In this case, Eq. (9) can be written as

$$P_{fa} = \frac{1}{2} - \frac{1}{2}\,\mathrm{erf}\left(\frac{\delta - \mu_{Y_o}}{\sqrt{2}\sigma_{Y_o}}\right) \tag{10}$$

where μ_{Y_o} and σ_{Y_o} are the out-of-lock mean and variance of the decision statistic Y. The threshold δ is given by

$$\delta = \sqrt{2}\sigma_{Y_o}\gamma + \mu_{Y_o} \tag{11}$$

where $\gamma = \mathrm{erf}^{-1}(1 - 2P_{fa})$. Substituting Eq. (11) into Eq. (6) relates the probability of detection to the no-signal (classical) false alarm rate, namely,

$$P_D = \frac{1}{2} - \frac{1}{2}\,\mathrm{erf}\left(\frac{\sqrt{2}\sigma_{Y_o}\gamma + \mu_{Y_o} - \mu_Y}{\sqrt{2}\sigma_Y}\right) \tag{12}$$

The next five subsections derive the in-lock and out-of-lock mean and variance for all five schemes.

A. Square-Law Lock Detector With Overlapping Intervals (SQOD)

The SQOD detector is shown in Fig. 2(a). For the input given by Eq. (1), the inphase integrator output is given by

$$I_k = \int_{kT+\tau}^{(k+1)T+\tau} r(t)dt$$

$$= d_k A(T-\tau) + d_{k+1}A\tau + N_1(k) + N_2(k) \tag{13}$$

and the quadraphase integrator output is given by

$$Q_k = \int_{(k+\frac{1}{2})T+\tau}^{(k+\frac{3}{2})T+\tau} r(t)dt$$

$$= \begin{cases} d_k A\left(\frac{T}{2}-\tau\right) + d_{k+1}A\left(\frac{T}{2}+\tau\right) & \\ \quad +N_2(k) + N_1(k+1) & 0 \le \tau < \frac{T}{2} \\ d_{k+1}A\left(\frac{3T}{2}-\tau\right) + d_{k+2}A\left(\tau - \frac{T}{2}\right) & \\ \quad +N_2(k) + N_1(k+1) & \frac{T}{2} \le \tau < T \end{cases} \tag{14}$$

where τ is limited to the interval $[0,\ T]$, and where

$$N_1(k) = \int_{(kT+\tau)}^{(k+\frac{1}{2})T+\tau} n(t)dt \tag{15}$$

and

$$N_2(k) = \int_{(k+\frac{1}{2})T+\tau}^{(k+1)T+\tau} n(t)dt \tag{16}$$

Since $n(t)$ is a white Gaussian process with one-sided PSD N_o, the N_i's are independent Gaussian random variables with a mean of zero and a variance of $\sigma_n^2 = (N_oT)/4$. Summing M of the samples $X_k = I_k^2 - Q_k^2$ yields Y. From Appendix A, the in-lock mean and variance of Y are given by

$$\mu_Y = \frac{\eta_s NoT}{2} \tag{17}$$

and

$$\sigma_Y^2 = \left(\frac{N_0T}{M}\right)^2 \left[M\left(\frac{\eta_s^2}{4} + 2\eta_s + \frac{3}{4}\right) + 2(M-1)\left(-\frac{\eta_s}{2} - \frac{1}{8}\right)\right] \quad (18)$$

The out-of-lock mean and variance, when there is a signal present and τ is an unknown constant over a decision interval $B_L = 1/(MT)$, are given by

$$\mu_{Y_o} = 0.0 \quad (19)$$

$$\sigma_{Y_o}^2 = \left(\frac{N_0T}{M}\right)^2 \left[M\left(\frac{31\eta_s^2}{120} + \frac{41\eta_s}{24} + \frac{3}{4}\right) + 2(M-1) \times \left(\frac{23\eta_s^2}{320} - \frac{23\eta_s}{48} - \frac{1}{8}\right) + (M-1)(M-2)\frac{\eta_s^2}{12}\right] \quad (20)$$

where η_s denotes the symbol signal-to-noise ratio and is defined as

$$\eta_s \triangleq \frac{A^2T}{N_0} \quad (21)$$

Setting $A = 0$ in Eq. (21) and substituting the result in Eqs. (19) and (20) yields the out-of-lock mean and variance in the no-signal case. Hence, the no-signal mean is zero, but the no-signal variance is given by

$$\sigma_{Y_o}^2(\eta_s = 0) = \left(\frac{N_0T}{M}\right)^2 \left[M\frac{3}{4} - 2(M-1)\frac{1}{8}\right] \quad (22)$$

B. Absolute-Value Lock Detector With Overlapping Intervals (AVOD)

For the AVOD detector, Fig. 2(a) with absolute values instead of squares, the expressions for I_k and Q_k given by Eqs. (13) and (14) are still valid, but now $X_k = |I_k| - |Q_k|$. From Appendix B, the in-lock mean and variance are given by

$$\mu_Y = \left(\sqrt{\frac{N_0T}{4}}\right)\left[\frac{\exp(-\eta_s) - 1}{\sqrt{\pi}} + \sqrt{\eta_s}\,\mathrm{erf}(\sqrt{\eta_s})\right] \quad (23)$$

and

$$\sigma_Y^2 = \frac{1}{M^2}[M\ \mathrm{Var}(X_k) + M(M-1)\ \mathrm{Cov}(X_k, X_{k+1})] \quad (24)$$

where

$$\mathrm{Var}(X_k) = (N_0T)\left\{\frac{3\eta_s}{2} + 1 - \eta_s[F_1(\eta_s) + F_2(\eta_s)] - \frac{1}{4\pi}[\exp(-2\eta_s) - 2\exp(-\eta_s) + 1] - \frac{\eta_s}{4}\mathrm{erf}^2(\sqrt{\eta_s}) - \frac{1}{2}\sqrt{\frac{\eta_s}{\pi}}\mathrm{erf}(\sqrt{\eta_s})[\exp(-\eta_s) - 1]\right\} \quad (25)$$

and

$$\mathrm{Cov}(X_k, X_{k+1}) = (N_0T)\left\{\frac{\exp(-2\eta_s) + \exp(-\eta_s)}{2\pi} + \frac{\eta_s}{2}\mathrm{erf}^2(\sqrt{\eta_s}) + \left[\exp(-\eta_s) + \frac{1}{2}\right]\mathrm{erf}(\sqrt{\eta_s}) \times\sqrt{\frac{\eta_s}{\pi}} - \frac{\eta_s}{2}[F_1(\eta_s) + F_2(\eta_s)]\right\} \quad (26)$$

The out-of-lock mean and variance, when there is a signal and τ is constant over M symbols, are given by

$$\mu_{Y_o} = 0.0 \quad (27)$$

and

$$\sigma_{Y_o}^2 = \frac{1}{M^2}[M\ \mathrm{Var}_o(X_k) + 2(M-1)\ \mathrm{Cov}_o(X_k, X_{k+1}) + (M-1)(M-2)\ \mathrm{Cov}_o(X_k, X_{k+2})] \quad (28)$$

where

$$\mathrm{Var}_o(X_k) = (N_0T)\left\{\frac{4\eta_s}{3} + 1 - \eta_s\left[\frac{3}{4}F_1(\eta_s) + G_1(\eta_s) + \frac{H_1(\eta_s) + H_2(\eta_s) + H_3(\eta_s)}{2}\right]\right\} \quad (29)$$

$$\mathrm{Cov}_o(X_k, X_{k+1}) = (N_0T)\left\{\frac{\exp(-2\eta_s)}{2\pi} + \left(\frac{\eta_s}{2} + \frac{1}{8}\right)\right.$$

$$\times \mathrm{erf}^2(\sqrt{\eta_s}) + \exp(-\eta_s)\mathrm{erf}(\sqrt{\eta_s})\left(\sqrt{\frac{\eta_s}{\pi}} + \frac{1}{8\sqrt{\pi\eta_s}}\right)$$

$$+\frac{\eta_s}{4}[F_3(\eta_s) + G_3(\eta_s) + H_4(\eta_s) - G_4(\eta_s) - H_5(\eta_s)$$

$$\left.-\frac{3}{2}F_1(\eta_s) - G_1(\eta_s) - 2G_2(\eta_s) - 2H_2(\eta_s)]\right\} \qquad (30)$$

$$\mathrm{Cov}_o(X_k, X_{k+j}) = \left(\frac{N_0T\eta_s}{4}\right)[F_3(\eta_s) + G_3(\eta_s) + H_4(\eta_s)$$

$$- 2G_4(\eta_s) - 2H_5(\eta_s)] \qquad \text{for j} \geq 2 \qquad (31)$$

The functions F_i, G_i, and H_i in Eqs. (28) through (31) are defined in Appendix B and plotted versus η_s in Fig. B-1. Setting $\eta_s = 0$ in Eqs. (28) through (31) yields the out-of-lock statistics in the no-signal case. The no-signal mean is zero, but the variance is given by

$$\sigma^2_{Y_o}(\eta_s = 0) = \left(\frac{N_0T}{M^2}\right)\left[M + 2(M-1)\left(\frac{1}{2\pi}\right)\right] \qquad (32)$$

C. Square-Law Lock Detector With Nonoverlapping Intervals (SQNOD)

The SQNOD detector is shown in Fig. 2(b). For the input of Eq. (1), The inphase and quadraphase integrator outputs are given by

$$I_k = \int_{(k+\frac{1}{4})T+\tau}^{(k+\frac{3}{4})T+\tau} r(t)dt$$

$$= \begin{cases} d_k\frac{AT}{2} + N_1(k) & 0 \leq \tau < \frac{T}{4} \\ d_kA\left(\frac{3T}{4} - \tau\right) & \\ \quad +d_{k+1}A\left(\tau - \frac{T}{4}\right) + N_1(k) & \frac{T}{4} \leq \tau < \frac{T}{2} \end{cases} \qquad (33)$$

and

$$Q_k = \int_{(k-\frac{1}{4})T+\tau}^{(k+\frac{1}{4})T+\tau} r(t)dt$$

$$= \begin{cases} d_{k-1}A\left(\frac{T}{4} - \tau\right) & \\ \quad +d_kA\left(\frac{T}{4} + \tau\right) + N_2(k) & 0 \leq \tau < \frac{T}{4} \\ d_k\frac{AT}{2} + N_2(k) & \frac{T}{4} \leq \tau < \frac{T}{2} \end{cases} \qquad (34)$$

The noises $N_1(k)$ and $N_2(k)$ are given by Eqs. (15) and (16) after changing the integration limits to those in Eqs. (33) and (34). As a result, they are independent Gaussian random variables with zero mean and variance $\sigma_n^2 = (N_0T)/4$. The sample X_k is the difference of the squares (i.e., $X_k = I_k^2 - Q_k^2$). From Appendix D, the in-lock mean and variance of Y are given by

$$\mu_Y = \frac{\eta_s N_0 T}{8} \qquad (35)$$

and

$$\sigma_Y^2 = \left(\frac{N_0^2T^2}{M}\right)\left(\frac{\eta_s^2 + 24\eta_s + 16}{64}\right) \qquad (36)$$

For the case of false lock with the signal present and where τ is an unknown constant over M symbols, one obtains

$$\mu_{Y_o} = 0.0 \qquad (37)$$

and

$$\sigma^2_{Y_o} = \left(\frac{N_0^2T^2}{M^2}\right)$$

$$\times\left[M\left(\frac{\eta_s^2 + 25\eta_s + 15}{60}\right) + M(M-1)\frac{\eta_s^2}{120}\right] \qquad (38)$$

When there is no signal present, the out-of-lock mean is zero and the variance is given by setting $\eta_s = 0$ in Eq. (38). Consequently, the no-signal out-of-lock variance is

$$\sigma^2_{Y_o}(\eta_s = 0) = \left(\frac{N_0^2T^2}{M}\right)\left(\frac{15}{60}\right) \qquad (39)$$

D. Absolute-Value Lock Detector With Disjoint Intervals (AVNOD)

This detector is the same as the SQNOD with the squaring operations replaced by absolute value operations. Hence, Eqs. (33) and (34) for I_k and Q_k are valid, but now

$X_k = |I_k| - |Q_k|$. From Appendix E, the in-lock statistics for Y are given by

$$\mu_Y = \sqrt{\frac{N_0T}{4}}\left[\frac{\exp\left(-\frac{\eta_s}{2}\right)-1}{\sqrt{2\pi}} + \frac{\sqrt{\eta_s}}{2}\mathrm{erf}\left(\sqrt{\frac{\eta_s}{2}}\right)\right] \quad (40)$$

and

$$\sigma_Y^2 = \left(\frac{N_0T}{M}\right)\left\{\frac{3\eta_s}{8} + \frac{1}{2} - \frac{1}{8\pi}\left[1 + 5\exp(-\eta_s) + 2\exp\left(-\frac{\eta_s}{2}\right)\right] - \sqrt{\frac{\eta_s}{32\pi}}\mathrm{erf}\left(\sqrt{\frac{\eta_s}{2}}\right) \times \left[5\exp\left(-\frac{\eta_s}{2}\right)+1\right] - \frac{5\eta_s}{16}\mathrm{erf}^2\left(\sqrt{\frac{\eta_s}{2}}\right)\right\} \quad (41)$$

The out-of-lock mean and variance when there is a signal present and τ is an unknown constant over MT sec are given by

$$\mu_{Y_o} = 0.0 \quad (42)$$

and

$$\sigma_{Y_o}^2 = \frac{1}{M^2}[M\ \mathrm{Var}_o(X_k) + M(M-1)\ \mathrm{Cov}_o(X_k, X_{k+1})] \quad (43)$$

$$\mathrm{Var}_o(X_k) = (N_0T)\left[\frac{5\eta_s}{12} + \frac{1}{2} - \frac{3}{4\pi}\exp(-\eta_s) - \mathrm{erf}^2\left(\sqrt{\frac{\eta_s}{2}}\right)\left(\frac{1+3\eta_s}{8}\right) - \exp\left(-\frac{\eta_s}{2}\right) \times \mathrm{erf}\left(\sqrt{\frac{\eta_s}{2}}\right)\left(\frac{3}{2}\sqrt{\frac{\eta_s}{2\pi}} + \frac{1}{\sqrt{32\pi\eta_s}}\right)\right] \quad (44)$$

$$\mathrm{Cov}_o(X_k, X_{k+1}) = (N_0T)\left\{-\frac{1}{16}\mathrm{erf}^2\left(\sqrt{\frac{\eta_s}{2}}\right) - \exp\left(-\frac{\eta_s}{2}\right) \times \mathrm{erf}\left(\sqrt{\frac{\eta_s}{2}}\right)\left(\frac{1}{8\sqrt{2\pi\eta_s}}\right) + \frac{\eta_s}{2}Z(\eta_s)\right\} \quad (45)$$

where the function Z is defined in Appendix E and plotted in Fig. B-2. For the out-of-lock case with no signal, the mean is zero and the variance is obtained by setting $\eta_s = 0$ in Eqs. (43) through (45). Hence, the out-of-lock variance is given by

$$\sigma_{Y_o}^2(\eta_s = 0) = \frac{N_0T}{M}\left(\frac{1}{2} - \frac{3}{4\pi}\right) \quad (46)$$

E. Signal-Power Estimator Lock Detector (SPED)

This detector is shown in Fig. 2(c). Denote the integrations over the first half of the assumed symbol interval as I_k and the second half as Q_k. Then, the I_k and Q_k samples are given by

$$I_k = d_k\frac{AT}{2} + N_1(k) \quad (47)$$

and

$$Q_k = d_kA\left(\frac{T}{2} - \tau\right) + d_{k+1}A\tau + N_2(k) \quad (48)$$

and $X_k = I_kQ_k$. From Appendix F, the in-lock mean and variance of Y are

$$\mu_Y = \frac{\eta_sN_0T}{4} \quad (49)$$

and

$$\sigma_Y^2 = \left(\frac{N_0^2T^2}{M}\right)\left(\frac{2\eta_s+1}{16}\right) \quad (50)$$

The out-of-lock case with signal present has a mean and variance, when τ is constant over M symbols, given by

$$\mu_{Y_o} = \frac{\eta_sN_0T}{8} \quad (51)$$

and

$$\sigma_{Y_o}^2 = \frac{N_0^2T^2}{M^2}\left[M\left(\frac{5\eta_s^2+20\eta_s+12}{192}\right) + M(M-1)\frac{\eta_s^2}{192}\right] \quad (52)$$

As before, the out-of-lock variance in the no-signal case is given by

$$\sigma^2_{Y_o}(\eta_s = 0) = \left(\frac{N_0^2 T^2}{M}\right)\left(\frac{12}{192}\right) \tag{53}$$

IV. Discussion and Simulation Results

Digital simulation was used to verify the foregoing analysis. The first part of this section presents the results for the long-time constant case or $B_L = 1/(MT)$. Simulation results for the short-time constant case or $B_L = 1/T$ are presented in Subsection IV.B. The last subsection discusses the no-signal case.

A. Long-Time Constant, $B_L = 1/(MT)$

In the out-of-lock state, the symbol timing error τ is modelled as a constant over a decision interval (MT sec), but it is independent and uniformly distributed over the collection of all decision intervals. The timing error in the in-lock state is modelled as being zero. Although the special case where τ is constant over M symbols was analyzed for performance comparison purposes, it is not advisable to operate a practical system under these conditions due to unacceptable false alarm rates. This case has higher than usual false alarm rates because the decision statistic for small values of τ is not significantly different from the statistic for $\tau = 0$. As a result, the out-of-lock states corresponding to small values of τ are frequently declared to be in-lock because they are mistaken for the case when $\tau = 0$. This problem can be ameliorated by lengthening the observation time relative to the time constant of τ (i.e., shortening the time constant of τ). In practice, it is recommended that the observation time be at least ten times longer than the time constant of τ.

As noted in Section II, the out-of-lock density function for Y in this case is not Gaussian. Consider the decision statistic Y when the loop is out-of-lock and τ is constant over M symbols. In general, it can be written as

$$X_k = s_k(\tau) + n_k + s_k(\tau)n_k \tag{54}$$

where (in all five cases) the signal term s_k is random and uniformly distributed because τ is a uniformly distributed random variable. The density of the noise n_k depends on the detector being implemented. Summing M samples of X_k (where X_k is at the symbol rate in all cases) yields the decision variable Y. Since τ is constant over the sum, at a high SNR (i.e., for strong signal levels) the density function of Y approaches a uniform distribution as shown in Fig. 3(a). However, at a low SNR the noise term dominates and the density of Y is Gaussian due to the central limit theorem, as shown in Fig. 3(b). The density in Fig. 3 was obtained via numerical integration, as well as simulation. Both methods are seen to agree very well. The numerical method computed the density function of Y and $f(y)$, by averaging over τ the conditional probability density function $f(y/\tau)$. The latter is Gaussian with mean and variance where both are functions of τ. The simulation method computed the histogram of Y and then set $f(y) = [P(y - \Delta \leq Y \leq y + \Delta)]/\Delta$, where Δ is the size of a histogram bin. The histograms were generated by using 1,000,000 symbols, which corresponds to 10,000 decisions (Y's), since there are 100 symbols/decision.

Figure 4 compares the probability of detection performance for all five detectors for $M = 100$ and $P_{fa} = 0.25$. Note that the overlapping detectors SQOD and AVOD, which are identical except for the squaring and absolute value operations, have nearly identical performances. As expected, the AVOD is slightly better at a high SNR, whereas the SQOD is slightly better at a low SNR. The nonoverlapping detectors SQNOD and AVNOD also have nearly equal performance. Once again, the absolute value operation yields better results at higher SNR's. The SPED is better than the nonoverlapping detectors, but worse than the overlapping detectors. The probability of detection results in Fig. 4 change when P_{fa} or M change. For example, increasing the observation interval increases the detection probability because it increases the detector SNR (μ_Y^2/σ_Y^2). Accepting a higher false alarm rate increases the probability of detection because it lowers the threshold δ. In generating these curves, 50,000 symbols were simulated for each value of SNR. Since there are 100 symbols/decision, the detection probability for a given SNR is based on 500 decisions.

B. Short-Time Constant, $B_L = 1/T$

Here, for the out-of-lock state, the symbol timing error τ is modelled as a uniformly distributed random variable that changes independently from symbol to symbol. For this case, the probabilities of detection for all five detectors are computed by simulation for $M = 100$ and $P_{fa} = 10^{-2}$, and the threshold δ is set according to Eq. (11). The false alarm rate was verified by simulation. The results are plotted versus the symbol energy-to-noise ratio η_s in Fig. 5. In these computer simulations, the detection probability for a given SNR is based on 40,000 decisions.

The results show that the AVOD performs slightly better than SQOD at a high SNR, whereas the AVOD and SQOD seem to perform identically at a low SNR. The nonoverlapping detectors SQNOD and AVNOD also have nearly equal performance at a low SNR, but AVNOD performs about 1 dB better for values of the symbol SNR

higher than −4 dB. The SPED performs about 2 dB worse than the overlapping detectors and 3 dB better than the other two nonoverlapping detectors.

Also by simulation, the false-alarm rate that was used in setting the threshold was verified.

C. No-Signal Case

This scenario distinguishes between the case when there is no signal and when there is a signal and $\tau = 0$. Clearly, the out-of-lock statistic is Gaussian with a zero mean, and the in-lock statistic is Gaussian with a nonzero mean. Probability of detection results are compared in Fig. 6. Interestingly, the performances of the overlapping and nonoverlapping schemes are grouped together, but the SPED now has the best performance. The interdependence among P_D, P_{fa}, and M is the same as in the other two cases.

V. Conclusion

The performances of five symbol lock detectors are compared in this article. These detectors are the square-law detector with overlapping and nonoverlapping integrators, the absolute value detectors with overlapping and nonoverlapping integrators, and the signal-power estimator detector. The analysis considered various scenarios in which the observation interval is much larger than or equal to the symbol synchronizer loop bandwidth, and which have not been considered in previous analyses. Also, the case of threshold setting in the absence of signal was considered.

It is shown that the SQOD outperforms all others when the threshold is set in the presence of signal, independent of the relationship between loop bandwidth and observation period. On the other hand, the SPED outperforms all others when the threshold is set in the presence of noise only.

Acknowledgments

The authors would like to thank A. Mileant for proposing the idea of disjoint intervals. Also, the valuable comments made by Dr. W. J. Hurd are greatly appreciated.

References

[1] S. Hinedi, "A Functional Description of the Advanced Receiver II," *TDA Progress Report 42-100*, vol. October–December 1989, Jet Propulsion Laboratory, Pasadena, California, pp. 131–149, February 15, 1990.

[2] A. Mileant and S. Hinedi, "Costas Loop Lock Detection in the Advanced Receiver," *TDA Progress Report 42-99*, vol. July–September 1989, Jet Propulsion Laboratory, Pasadena, California, pp. 72–89, November 15, 1989.

[3] A. Mileant and S. Hinedi, "QPSK Loop Lock Detection in the Advanced Receiver," *TDA Progress Report 42-99*, vol. July–September 1989, Jet Propulsion Laboratory, Pasadena, California, pp. 72–89, November 15, 1989.

[4] J. K. Holmes, *Coherent Spread Spectrum System*, New York: John Wiley and Sons, 1982.

[5] K. T. Woo, *Shuttle Bit Synch Lock Detector Performance*, TRW IOC No. SCTE-50-76-184/KTW, TRW Corporation, El Segundo, California, April 5, 1976.

[6] M. Simon, "An Analysis of the Steady-State Phase Noise Performance of a Digital Data-Transition Tracking Loop," *JPL Space Programs Summary 37-55*, vol. 3, Jet Propulsion Laboratory, Pasadena, California, pp. 54–62, February 28, 1969.

[7] M. Simon and A. Mileant, "SNR Estimation for the Baseband Assembly," *TDA Progress Report 42-85*, vol. January–March 1986, Jet Propulsion Laboratory, Pasadena, California, pp. 118–125, May 15, 1986.

[8] D. Fraser, *Non-Parametric Methods in Statistics*, New York: John Wiley and Sons, 1957.

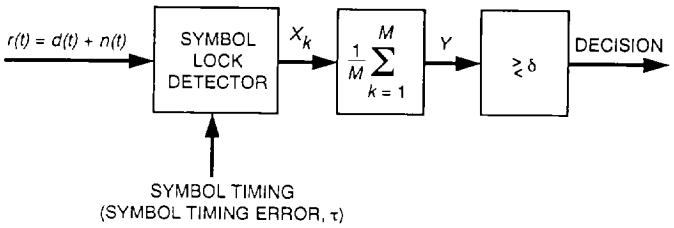

Fig. 1. Signal-processing functions common to all five lock detectors.

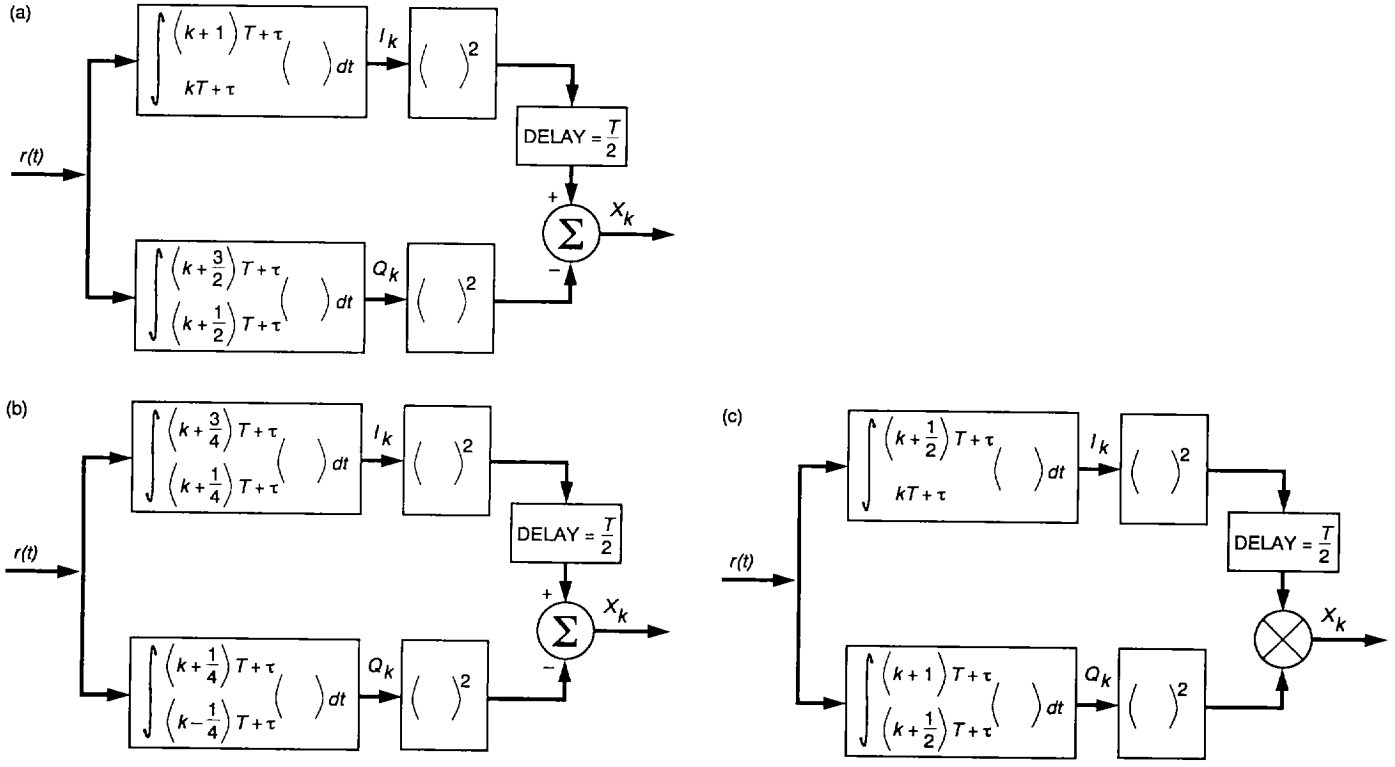

Fig. 2. Three of the detectors: (a) the SQOD, replacing $(\ )^2$ with 11 yields the absolute-value detector AVOD), (b) the SQNOD, replacing $(\ )^2$ with 11 yields the absolute-value detector AVNOD, and (c) the SPED.

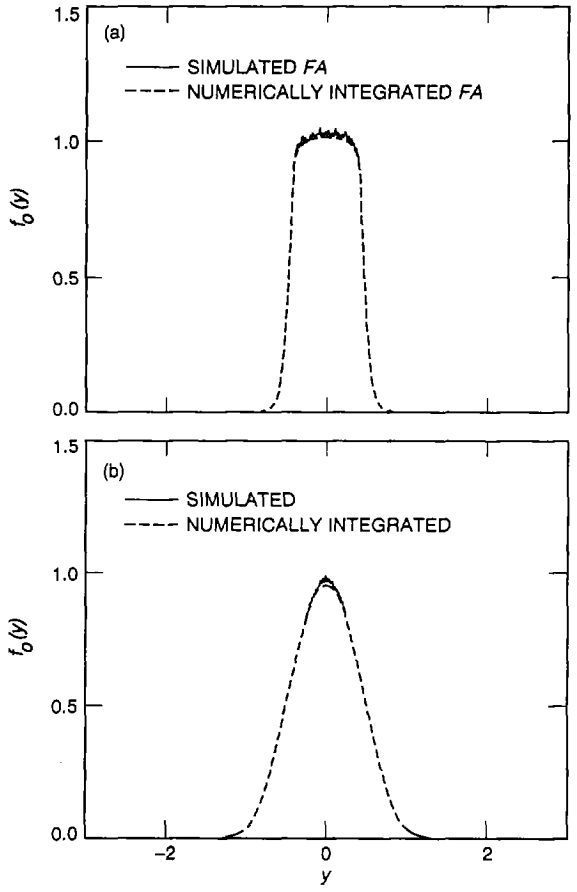

Fig. 3. The probability density function of Y for the SQOD, when the loop is out of lock, has a: (a) high SNR = 5 dB and (b) low SNR = −5 dB.

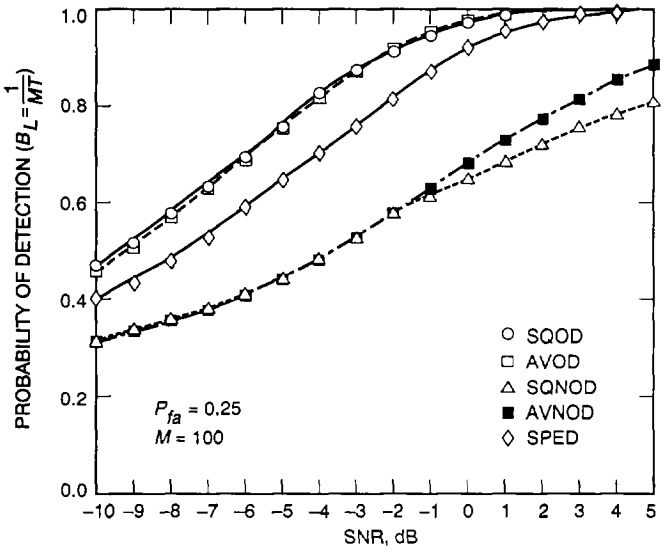

Fig. 4. The probability of detection versus SNR when τ is an unknown constant over a decision interval.

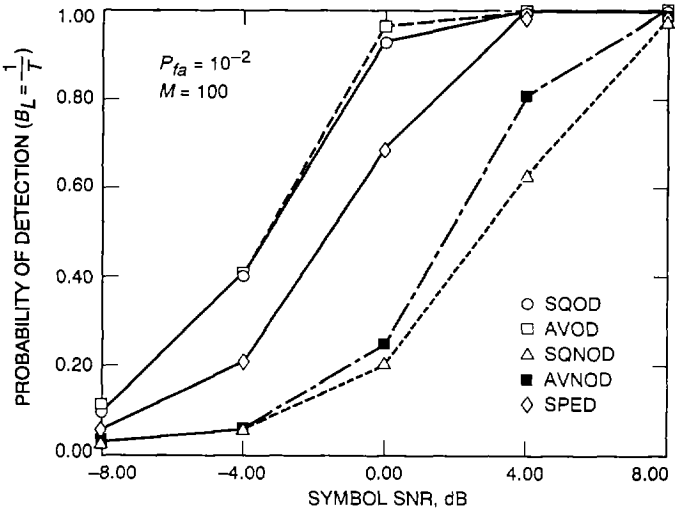

Fig. 5. The probability of detection versus SNR when τ is uniformly distributed and charging from symbol to symbol.

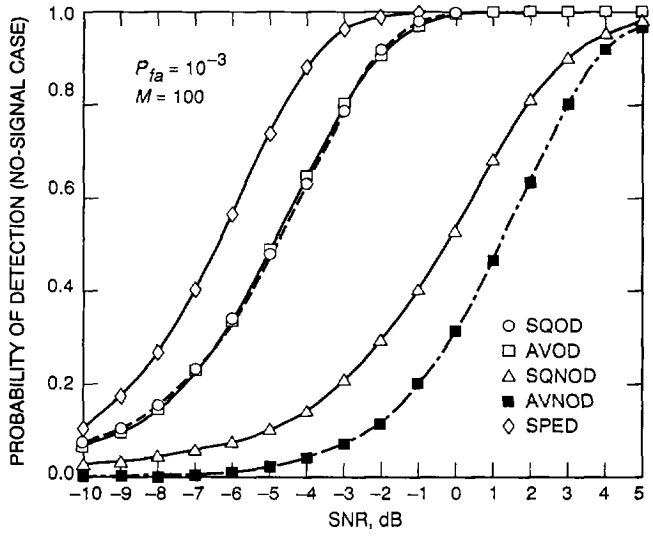

Fig. 6. The probability of detection versus SNR when the false alarm rate is computed in the absence of a signal.

Appendix A

Derivation of the Mean and Variance of the SQOD

The inphase and quadraphase integrator outputs are given by Eqs. (13) and (14), respectively. The output of the lock detector $X_k = I_k^2 - Q_k^2$. Consequently,

$$\mu_k = \mathcal{E}\{I_k^2\} - \mathcal{E}\{Q_k^2\} \tag{A-1}$$

where $\mu_k = \mathcal{E}\{X_k\}$.

$$\begin{aligned} \mathrm{Var}(X_k) &= \mathcal{E}\{[I_k^2 - Q_k^2]^2\} - \mathcal{E}^2\{I_k^2 - Q_k^2\} \\ &= \mathcal{E}\{I_k^4 + Q_k^4 - 2I_k^2Q_k^2\} - \mu_k^2 \end{aligned} \tag{A-2}$$

The covariance of X_k with X_{k+j} is

$$\mathrm{Cov}(X_k, X_{k+j}) = \mathcal{E}\{I_k^2 I_{k+1}^2\} + \mathcal{E}\{Q_k^2 Q_{k+j}^2\} - \mathcal{E}\{I_k^2 Q_{k+j}^2\} - \mathcal{E}\{I_{k+j}^2 Q_k^2\} - \mu_k \mu_{k+j} \tag{A-3}$$

When the loop is in lock, Eqs. (A-1) through (A-3) are evaluated with τ set to zero in Eqs. (A-10) through (A-18). Hence, the in-lock moments of X_k are given by

$$\mathrm{Var}(X_k) = \frac{A^4T^4}{4} + 8A^2T^2\sigma_n^2 + 12\sigma_n^4 \tag{A-4}$$

and

$$\mathrm{Cov}(X_k, X_{k+1}) = -2A^2T^2\sigma_n^2 - 2\sigma_n^4 \tag{A-5}$$

and for $j \geq 2$, this can be shown to be

$$\mathrm{Cov}(X_k, X_{k+j}) = 0 \tag{A-6}$$

When the loop is out-of-lock, τ is modelled as a uniform random variable. Using this model for τ in Eqs. (A-10) through (A-18) and substituting the results into Eqs. (A-1) through (A-3) give the out-of-lock moments of X_k. Namely, (where the additional subscript o denotes out-of-lock),

$$\mathrm{Var}_o(I_k^2 - Q_k^2) = \frac{31A^4T^4}{120} + \frac{41}{6}A^2T^2\sigma_n^2 + 12\sigma_n^4 \tag{A-7}$$

$$\mathrm{Cov}_o(X_k, X_{k+1}) = \frac{23A^4T^4}{320} - \frac{23}{12}A^2T^2\sigma_n^2 - 2\sigma_n^4 \tag{A-8}$$

and for $j \geq 2$, this can be shown to be

$$\mathrm{Cov}_o(X_k, X_{k+j}) = \frac{A^4T^4}{12} \tag{A-9}$$

The following equations were used to compute the variance of X_k and covariance of X_k with X_{k+1}:

$$\mathcal{E}\{I_k^2\} = A^2(T^2 - 2T\mathcal{E}\{\tau\} + 2\mathcal{E}\{\tau^2\}) + 2\sigma_n^2 \tag{A-10}$$

$$\mathcal{E}\{Q_k^2\} = \begin{cases} A^2(\frac{T^2}{2}\mathcal{E}_1\{1\} + 2\mathcal{E}_1\{\tau^2\}) + 2\sigma_n^2\mathcal{E}_1\{1\} & 0 \le \tau < \frac{T}{2} \\ A^2(\frac{5T^2}{2}\mathcal{E}_2\{1\} - 4T\mathcal{E}_2\{\tau\} + 2\mathcal{E}_2\{\tau^2\}) + 2\sigma_n^2\mathcal{E}_2\{1\} & \frac{T}{2} \le \tau < T \end{cases} \tag{A-11}$$

$$\mathcal{E}\{I_k^4\} = A^4(T^4 - 4T^3\mathcal{E}\{\tau\} + 12T^2\mathcal{E}\{\tau^2\} - 16T\mathcal{E}\{\tau^3\} + 8\mathcal{E}\{\tau^4\}) + A^2\sigma_n^2(12T^2 - 24T\mathcal{E}\{\tau\} + 24\mathcal{E}\{\tau^2\}) + 12\sigma_n^4 \tag{A-12}$$

$$\mathcal{E}\{Q_k^4\} = \begin{cases} A^4(\frac{T^4}{2}\mathcal{E}_1\{1\} + 8\mathcal{E}_1\{\tau^4\}) & \\ \quad +A^2\sigma_n^2(6T^2\mathcal{E}_1\{1\} + 24\mathcal{E}_1\{\tau^2\}) + 12\sigma_n^4\mathcal{E}_1\{1\} & 0 \le \tau < \frac{T}{2} \\ A^4(\frac{17T^4}{2}\mathcal{E}_2\{1\} - 32T^3\mathcal{E}_2\{\tau\} + 48T^2\mathcal{E}_2\{\tau^2\} - 32T\mathcal{E}_2\{\tau^3\} + 8\mathcal{E}_2\{\tau^4\}) & \\ \quad +A^2\sigma_n^2(30T^2\mathcal{E}_2\{1\} - 48T\mathcal{E}_2\{\tau\} + 24\mathcal{E}_2\{\tau^2\}) + 12\sigma_n^4\mathcal{E}_2\{1\} & \frac{T}{2} \le \tau < T \end{cases} \tag{A-13}$$

$$\mathcal{E}\{I_k^2Q_k^2\} = \begin{cases} A^4(\frac{T^4}{2}\mathcal{E}_1\{1\} + 2T^2\mathcal{E}_1\{\tau^2\} - 8T\mathcal{E}_1\{\tau^3\} + 8\mathcal{E}_1\{\tau^4\}) & \\ \quad +A^2\sigma_n^2(5T^2\mathcal{E}_1\{1\} - 8T\mathcal{E}_1\{\tau\} + 16\mathcal{E}_1\{\tau^2\}) + 6\sigma_n^4\mathcal{E}_1\{1\} & 0 \le \tau < \frac{T}{2} \\ A^4(\frac{5T^4}{2}\mathcal{E}_2\{1\} - 9T^3\mathcal{E}_2\{\tau\} + 15T^2\mathcal{E}_2\{\tau^2\} - 12T\mathcal{E}_2\{\tau^3\} + 4\mathcal{E}_2\{\tau^4\}) & \\ \quad +A^2\sigma_n^2(7T^2\mathcal{E}_2\{1\} - 6T\mathcal{E}_2\{\tau\} + 4\mathcal{E}_2\{\tau^2\}) + 6\sigma_n^4\mathcal{E}_2\{1\} & \frac{T}{2} \le \tau < T \end{cases} \tag{A-14}$$

$$\mathcal{E}\{I_k^2I_{k+1}^2\} = A^4(T^4 - 4T^3\mathcal{E}\{\tau\} + 8T^2\mathcal{E}\{\tau^2\} - 8T\mathcal{E}\{\tau^3\} + 4\mathcal{E}\{\tau^4\}) + A^2\sigma_n^2(4T^2 - 8T\mathcal{E}\{\tau\} + 8\mathcal{E}\{\tau^2\}) + 4\sigma_n^4 \tag{A-15}$$

$$\mathcal{E}\{Q_k^2Q_{k+1}^2\} = \begin{cases} A^4(\frac{T^4}{4}\mathcal{E}_1\{1\} + 2T^2\mathcal{E}_1\{\tau^2\} + 4\mathcal{E}_1\{\tau^4\}) & \\ \quad +A^2\sigma_n^2(2T^2\mathcal{E}_1\{1\} + 8\mathcal{E}_1\{\tau^2\}) + 4\sigma_n^4\mathcal{E}_1\{1\} & 0 \le \tau < \frac{T}{2} \\ A^4(\frac{25T^4}{4}\mathcal{E}_2\{1\} - 20T^3\mathcal{E}_2\{\tau\} + 26T^2\mathcal{E}_2\{\tau^2\} - 16T\mathcal{E}_2\{\tau^3\} + 4\mathcal{E}_2\{\tau^4\}) & \\ \quad +A^2\sigma_n^2(10T^2\mathcal{E}_2\{1\} - 16T\mathcal{E}_2\{\tau\} + 8\mathcal{E}_2\{\tau^2\}) + 4\sigma_n^4\mathcal{E}_2\{1\} & \frac{T}{2} \le \tau < T \end{cases} \tag{A-16}$$

$$\mathcal{E}\{I_k^2 Q_{k+1}^2\} = \begin{cases} A^4(\frac{T^4}{2}\mathcal{E}_1\{1\} - T^3\mathcal{E}_1\{\tau\} + 3T^2\mathcal{E}_1\{\tau^2\} - 4T\mathcal{E}_1\{\tau^3\} + 4\mathcal{E}_1\{\tau^4\}) & \\ \quad +A^2\sigma_n^2(3T^2\mathcal{E}_1\{1\} - 4T\mathcal{E}_1\{\tau\} + 8\mathcal{E}_1\{\tau^2\}) + 4\sigma_n^4\mathcal{E}_1\{1\} & 0 \le \tau < \frac{T}{2} \\ A^4(\frac{5T^4}{2}\mathcal{E}_2\{1\} - 9T^3\mathcal{E}_2\{\tau\} + 15T^2\mathcal{E}_2\{\tau^2\} - 12T\mathcal{E}_2\{\tau^3\} + 4\mathcal{E}_2\{\tau^4\}) & \\ \quad +A^2\sigma_n^2(7T^2\mathcal{E}_2\{1\} - 12T\mathcal{E}_2\{\tau\} + 8\mathcal{E}_2\{\tau^2\}) + 4\sigma_n^4\mathcal{E}_2\{1\} & \frac{T}{2} \le \tau < T \end{cases} \tag{A-17}$$

$$\mathcal{E}\{I_{k+1}^2 Q_k^2\} = \begin{cases} A^4(\frac{T^4}{2}\mathcal{E}_1\{1\} - T^3\mathcal{E}_1\{\tau\} + 3T^2\mathcal{E}_1\{\tau^2\} - 4T\mathcal{E}_1\{\tau^3\} + 4\mathcal{E}_1\{\tau^4\}) & \\ \quad +A^2\sigma_n^2(5T^2\mathcal{E}_1\{1\} - 2T\mathcal{E}_1\{\tau\} + 4\mathcal{E}_1\{\tau^2\}) + 6\sigma_n^4\mathcal{E}_1\{1\} & 0 \le \tau < \frac{T}{2} \\ A^4(\frac{5T^4}{2}\mathcal{E}_2\{1\} - \frac{39T^3}{4}\mathcal{E}_2\{\tau\} + \frac{71T^2}{4}\mathcal{E}_2\{\tau^2\} - 15T\mathcal{E}_2\{\tau^3\} + 5\mathcal{E}_2\{\tau^4\}) & \\ \quad +A^2\sigma_n^2(13T^2\mathcal{E}_2\{1\} - 24T\mathcal{E}_2\{\tau\} + 16\mathcal{E}_2\{\tau^2\}) + 6\sigma_n^4\mathcal{E}_2\{1\} & \frac{T}{2} \le \tau < T \end{cases} \tag{A-18}$$

where, in the above equations

$$\mathcal{E}\{f(\tau)\} \triangleq \int_0^T f(\tau)p(\tau)d\tau \tag{A-19}$$

$$\mathcal{E}_1\{f(\tau)\} \triangleq \int_0^{\frac{T}{2}} f(\tau)p(\tau)d\tau \tag{A-20}$$

$$\mathcal{E}_2\{f(\tau)\} \triangleq \int_{\frac{T}{2}}^T f(\tau)p(\tau)d\tau \tag{A-21}$$

where $p(\tau)$ is the probabilty density function of the variable τ.

Appendix B

Derivation of the Mean and Variance of the AVOD

Note that the calculations in this appendix incorportate the results of Appendix C. The inphase and quadraphase outputs are given, respectively, by Eqs. (13) and (14). The lock detector output $X_k = |I_k| - |Q_k|$. Let $\mu_k = \mathcal{E}\{|I_k| - |Q_k|\}$. Then,

$$\begin{aligned} \mathrm{Var}(X_k) &= \mathcal{E}\{[|I_k| - |Q_k|]^2\} - \mu_k^2 \\ &= \mathcal{E}\{I_k^2 + Q_k^2 - 2|I_k Q_k|\} - \mu_k^2 \end{aligned} \tag{B-1}$$

and

$$\begin{aligned} \mathrm{Cov}(X_k, X_{k+j}) &= \mathcal{E}\{[|I_k| - |Q_k| - \mu_k][|I_{k+j}| - |Q_{k+j}| - \mu_{k+j}]\} \\ &= \mathcal{E}\{|I_k I_{k+j}|\} + \mathcal{E}\{|Q_k Q_{k+j}|\} - \mathcal{E}\{|I_k Q_{k+j}|\} - \mathcal{E}\{|I_{k+j} Q_k|\} - \mu_k \mu_{k+j} \end{aligned} \tag{B-2}$$

The following equations were used to compute the variance of X_k and the covariance of X_k with X_{k+1}:

$$\mathcal{E}\{X_k\} = \begin{cases} \frac{1}{2}[\mathcal{E}_1\{|AT - 2A\tau + N|\} - \mathcal{E}_1\{|2A\tau + N|\}] & 0 \le \tau < \frac{T}{2} \\ \frac{1}{2}[\mathcal{E}_2\{|AT - 2A\tau + N|\} - \mathcal{E}_2\{|2AT - 2A\tau + N|\}] & \frac{T}{2} \le \tau < T \end{cases} \tag{B-3}$$

$$\mathcal{E}\{|I_k Q_k|\} = \begin{cases} \frac{1}{2}[\mathcal{E}_1\{|[AT + N_1(k) + N_2(k)][AT + N_2(k) + N_1(k+1)]|\} \\ \quad +\mathcal{E}_1\{|[AT - 2A\tau + N_1(k) + N_2(k)][-2A\tau + N_2(k) + N_1(k+1)]|\}] & 0 \le \tau < \frac{T}{2} \\ \frac{1}{4}[\mathcal{E}_2\{|[AT + N_1(k) + N_2(k)][AT + N_2(k) + N_1(k+1)]|\} \\ \quad +\mathcal{E}_2\{|[AT + N_1(k) + N_2(k)][2AT - 2A\tau + N_2(k) + N_1(k+1)]|\} \\ \quad +\mathcal{E}_2\{|[AT - 2A\tau + N_1(k) + N_2(k)][2AT - 2A\tau + N_2(k) + N_1(k+1)]|\} \\ \quad +\mathcal{E}_2\{|[AT - 2A\tau + N_1(k) + N_2(k)][AT + N_2(k) + N_1(k+1)]|\}] & \frac{T}{2} \le \tau < T \end{cases} \tag{B-4}$$

$$\begin{aligned} \mathcal{E}\{|I_k I_{k+1}|\} = \frac{1}{4}[&\mathcal{E}^2\{|AT + N_1(k) + N_2(k)|\} \\ &+ \mathcal{E}\{|[AT - 2A\tau + N_1(k) + N_2(k)][AT - 2A\tau + N_1(k+1) + N_2(k+1)]|\} \\ &+ 2\mathcal{E}\{|AT + N_1(k) + N_2(k)|\}\mathcal{E}\{|AT - 2A\tau + N_1(k+1) + N_2(k+1)|\}] \end{aligned} \tag{B-5}$$

$$\mathcal{E}\{|Q_kQ_{k+1}|\} = \begin{cases} \frac{1}{4}[\mathcal{E}_1^2\{|AT+N_1+N_2|\} + \mathcal{E}_1\{|[2A\tau + N_1(k+1) + N_2(k)] \\ \quad \times [2A\tau + N_1(k+2) + N_2(k+1)]|\} \\ \quad +2\mathcal{E}\{|AT+N_1+N_2|\}\mathcal{E}_1\{|2A\tau + N_1 + N_2|\}] & 0 \le \tau < \frac{T}{2} \\ \frac{1}{4}[\mathcal{E}_2^2\{|AT+N_1+N_2|\} + \mathcal{E}_2\{|[2AT - 2A\tau + N_1(k+1) + N_2(k)] \\ \quad \times [2AT - 2A\tau + N_1(k+2) + N_2(k+1)]|\} \\ \quad +2\mathcal{E}\{|AT+N_1+N_2|\}\mathcal{E}_2\{|2AT - 2A\tau + N_1 + N_2|\}] & \frac{T}{2} \le \tau < T \end{cases} \tag{B-6}$$

$$\mathcal{E}\{|I_kQ_{k+1}|\} = \begin{cases} \frac{1}{4}[\mathcal{E}^2\{|AT+N_1+N_2|\} + \mathcal{E}_1\{|[2A\tau + N_1(k+1) + N_2(k)] \\ \quad \times [AT - 2A\tau + N_1(k+2) + N_2(k+1)]|\} \\ \quad +2\mathcal{E}\{|AT+N_1+N_2|\}\mathcal{E}_1\{|2A\tau + N_1 + N_2|\}] & 0 \le \tau < \frac{T}{2} \\ \frac{1}{4}[\mathcal{E}^2\{|AT+N_1+N_2|\} + \mathcal{E}_2\{|[AT - 2A\tau + N_1(k+1) + N_2(k)] \\ \quad \times [2AT - 2A\tau + N_1(k+2) + N_2(k+1)]|\} \\ \quad +2\mathcal{E}\{|AT+N_1+N_2|\}\mathcal{E}\{|AT - 2A\tau + N_1 + N_2|\}] & \frac{T}{2} \le \tau < T \end{cases} \tag{B-7}$$

$$\mathcal{E}\{|I_{k+1}Q_k|\} = \begin{cases} \frac{1}{4}[\mathcal{E}_1\{|[AT + N_1(k+1) + N_2(k+1)][AT + N_1(k+1) + N_2(k)]|\} \\ \quad +\mathcal{E}_1\{|[AT - 2A\tau + N_1(k+1) + N_2(k+1)][AT + N_1(k+1) + N_2(k)]|\} \\ \quad +\mathcal{E}_1\{|[AT - 2A\tau + N_1(k+1) + N_2(k+1)][2A\tau + N_1(k+1) + N_2(k)]|\} \\ \quad +\mathcal{E}_1\{|[AT + N_1(k+1) + N_2(k+1)][2A\tau + N_1(k+1) + N_2(k)]|\}] & 0 \le \tau < \frac{T}{2} \\ \frac{1}{2}[\mathcal{E}_2\{|[AT - 2A\tau + N_1(k+1) + N_2(k+1)][2AT - 2A\tau + N_1(k+1) + N_2(k)]|\} \\ \quad +\mathcal{E}_2\{|[AT + N_1(k+1) + N_2(k+1)][AT + N_1(k+1) + N_2(k)]|\}] & \frac{T}{2} \le \tau < T \end{cases} \tag{B-8}$$

where $\mathcal{E}_1$ and $\mathcal{E}_2$ are defined in Appendix A. The following functions were defined to obtain the results in Subsection III.A of the main text.

$$F_1(\eta_s) \triangleq \mathcal{E}\{|(1 + cn_1 + cn_2)(1 + cn_2 + cn_3)|\}$$

$$F_2(\eta_s) \triangleq \mathcal{E}\{|(1 + cn_1 + cn_2)(cn_2 + cn_3)|\}$$

$$F_3(\eta_s) \triangleq \mathcal{E}\{|(1 - 2u + cn_1 + cn_2)(1 - 2u + cn_3 + cn_4)|\}$$

$$G_1(\eta_s) \triangleq \mathcal{E}_1\{|(1 - 2u + cn_1 + cn_2)(2u + cn_2 + cn_3)|\}$$

$$G_2(\eta_s) \triangleq \mathcal{E}_1\{|(1 - 2u + cn_1 + cn_2)(1 + cn_2 + cn_3)|\}$$

$$G_3(\eta_s) \triangleq \mathcal{E}_1\{|(2u + cn_1 + cn_2)(2u + cn_3 + cn_4)|\}$$

$$G_4(\eta_s) \triangleq \mathcal{E}_1\{|(2u + cn_1 + cn_2)(1 - 2u + cn_3 + cn_4)|\}$$

$$H_1(\eta_s) \triangleq \mathcal{E}_2\{|(1 + cn_1 + cn_2)(2 - 2u + cn_2 + cn_3)|\}$$

$$H_2(\eta_s) \triangleq \mathcal{E}\{|(1 - 2u + cn_1 + cn_2)(2 - 2u + cn_2 + cn_3)|\}$$

$$H_3(\eta_s) \triangleq \mathcal{E}\{|(1 - 2u + cn_1 + cn_2)(1 + cn_2 + cn_3)|\}$$

$$H_4(\eta_s) \triangleq \mathcal{E}\{|(2 - 2u + cn_1 + cn_2)(2 - 2u + cn_3 + cn_4)|\}$$

$$H_5(\eta_s) \triangleq \mathcal{E}\{|(1 - 2u + cn_1 + cn_2)(2 - 2u + cn_3 + cn_4)|\} \tag{B-9}$$

where $c \triangleq 1/(2\sqrt{\eta_s})$, the n_i's are normal independent random variables with zero mean and unit variance, and u is a uniform random variable in the range $[0, 1]$. In Fig. B-1, one plots these functions versus η_s. These functions have been computed as follows: In the F functions, the expectation with respect to u is carried over the entire region [0, 1], while in G and H functions, the expectation is carried over [0, 1/2] and [1/2, 1], respectively.

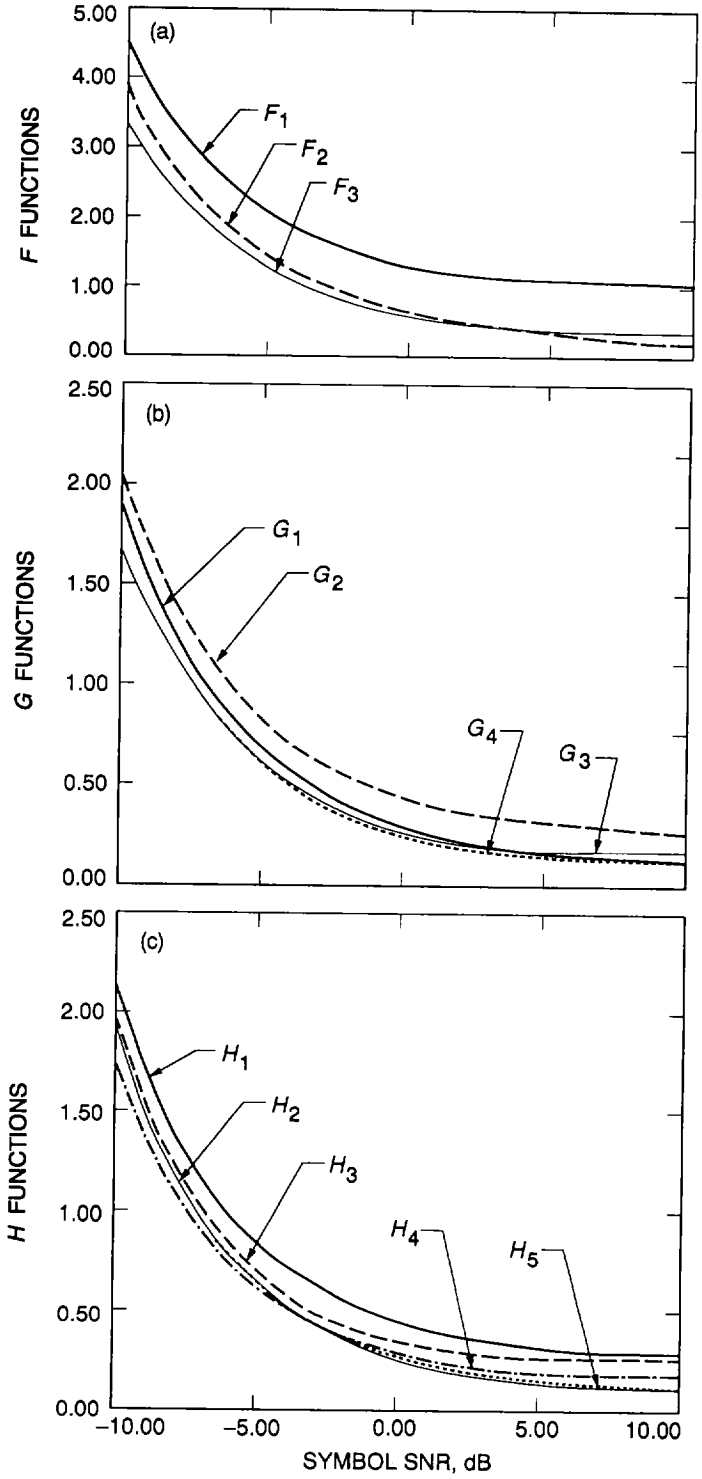

Fig. B-1. Function versus symbol SNR for: (a) *F* functions, (b) *G* functions, and (c) *H* functions.

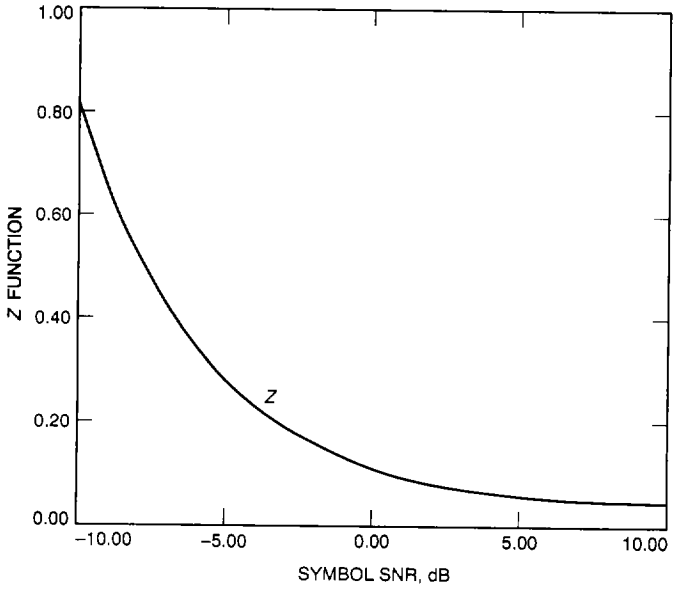

Fig. B-2. *Z* function versus symbol SNR.

Appendix C

Derivation of the Mean for the Random Variable $|n + b\tau + c|$

Let n be a normal random variable with zero mean and variance σ^2, τ a uniform random variable over $(0, T)$, and c any constant. Then,

$$\mathcal{E}\{|n+c|\} = \frac{1}{\sqrt{2\pi\sigma^2}} \int_{-\infty}^{\infty} |n+c| \exp\left(-\frac{n^2}{2\sigma^2}\right) dn \tag{C-1}$$

The above integral can be easily evaluated by breaking it into two integrals over the two regions $(-\infty, -c)$ and $(-c, \infty)$ to obtain

$$\mathcal{E}\{|n+c|\} = \sqrt{\frac{2\sigma^2}{\pi}} \exp\left(-\frac{c^2}{2\sigma^2}\right) + c \operatorname{erf}\left(\frac{c}{\sqrt{2\sigma^2}}\right) \tag{C-2}$$

For a fixed τ, one can write

$$\mathcal{E}\{|n+b\tau+c|\} = \sqrt{\frac{2\sigma^2}{\pi}} \exp\left(-\frac{(b\tau+c)^2}{2\sigma^2}\right) + (b\tau+c)\operatorname{erf}\left(\frac{b\tau+c}{\sqrt{2\sigma^2}}\right) \tag{C-3}$$

Unconditioning over τ yields

$$\mathcal{E}_1\{|n+b\tau+c|\} = \frac{1}{T}\int_0^{\frac{T}{2}} \left[\sqrt{\frac{2\sigma^2}{\pi}} \exp\left(-\frac{(b\tau+c)^2}{2\sigma^2}\right) + (b\tau+c)\operatorname{erf}\left(\frac{b\tau+c}{\sqrt{2\sigma^2}}\right)\right] d\tau \tag{C-4}$$

which, after integration by parts, leads to

$$\mathcal{E}_1\{|n+b\tau+c|\} = \frac{\sigma^2}{2bT}\left[\operatorname{erf}\left(\frac{\frac{bT}{2}+c}{\sqrt{2\sigma^2}}\right) - \operatorname{erf}\left(\frac{c}{\sqrt{2\sigma^2}}\right)\right] + \frac{1}{2bT}\left[\left(\frac{bT}{2}+c\right)^2 \operatorname{erf}\left(\frac{\frac{bT}{2}+c}{\sqrt{2\sigma^2}}\right) - c^2\operatorname{erf}\left(\frac{c}{\sqrt{2\sigma^2}}\right)\right]$$

$$+ \sqrt{\frac{\sigma^2}{2\pi}}\frac{1}{bT}\left[\left(\frac{bT}{2}+c\right)\exp\left(\frac{-(\frac{bT}{2}+c)^2}{2\sigma^2}\right) - c\exp\left(\frac{-c^2}{2\sigma^2}\right)\right] \tag{C-5}$$

By applying the above expression, one gets

$$\mathcal{E}_1\{|AT - 2A\tau + N_1 + N_2|\} = \sqrt{N_0 T}\left[\frac{1}{8\sqrt{\eta_s}}\operatorname{erf}(\sqrt{\eta_s}) + \frac{\sqrt{\eta_s}}{4}\operatorname{erf}(\sqrt{\eta_s}) + \frac{1}{4\sqrt{\pi}}\exp(-\eta_s)\right] \tag{C-6}$$

Also, by simple manipulation, it can be shown that

$$\begin{aligned}\mathcal{E}_1\{|AT - 2A\tau + N_1 + N_2|\} &= \mathcal{E}_2\{|AT - 2A\tau + N_1 + N_2|\} \\ &= \mathcal{E}_1\{|2A\tau + N_1 + N_2|\} \\ &= \mathcal{E}_2\{|2AT - 2A\tau + N_1 + N_2|\}\end{aligned} \tag{C-7}$$

Appendix D
Derivation of the Mean and Variance of the SQNOD

The samples I_k and Q_k are given by Eqs. (33) and (34). The moments of X_k are given by Eqs. (A-1) through (A-3). Using Eqs. (D-7) through (D-10) with $\tau = 0$ and Eqs. (A-2) and (A-3) yields the in-lock variance. Namely,

$$\mathrm{Var}(X_k) = \frac{A^4T^4}{64} + \frac{3}{2}A^2T^2\sigma_n^2 + 4\sigma_n^4 \tag{D-1}$$

The covariance can be shown to be, for $j \geq 1$,

$$\mathrm{Cov}(X_k, X_{k+j}) = 0 \tag{D-2}$$

Similarly, with τ modelled as uniform over $[0,\ T/2]$ in Eqs. (D-7) through (D-10), the out-of-lock moments are found. Hence,

$$\mathrm{Var}_o(X_k) = \frac{A^4T^4}{60} + \frac{5}{3}A^2T^2\sigma_n^2 + 4\sigma_n^4 \tag{D-3}$$

The out-of-lock covariance can be shown to be, for $j \geq 1$,

$$\mathrm{Cov}_o(X_k, X_{k+j}) = \frac{A^4T^4}{120} \tag{D-4}$$

The following equations are used in computing the variance of X_k:

$$\mathcal{E}\{I_k^2\} = \begin{cases} (\frac{A^2T^2}{4} + \sigma_n^2)\mathcal{E}_1\{1\} & 0 \leq \tau < \frac{T}{4} \\ A^2(\frac{5T^2}{8}\mathcal{E}_2\{1\} - 2T\mathcal{E}_2\{\tau\} + 2\mathcal{E}_2\{\tau^2\}) + \sigma_n^2\mathcal{E}_2\{1\} & \frac{T}{4} \leq \tau < \frac{T}{2} \end{cases} \tag{D-5}$$

$$\mathcal{E}\{Q_k^2\} = \begin{cases} A^2(\frac{T^2}{8}\mathcal{E}_1\{1\} + 2\mathcal{E}_1\{\tau^2\}) + \sigma_n^2\mathcal{E}_1\{1\} & 0 \leq \tau < \frac{T}{4} \\ (\frac{A^2T^2}{4} + \sigma_n^2)\mathcal{E}_2\{1\} & \frac{T}{4} \leq \tau < \frac{T}{2} \end{cases} \tag{D-6}$$

$$\mathcal{E}\{I_k^4\} = \begin{cases} (\frac{A^4T^4}{16} + \frac{3}{2}A^2T^2\sigma_n^2 + 3\sigma_n^4)\mathcal{E}_1\{1\} & 0 \leq \tau < \frac{T}{4} \\ A^4(\frac{17T^4}{32}\mathcal{E}_2\{1\} - 4T^3\mathcal{E}_2\{\tau\} + 12T^2\mathcal{E}_2\{\tau^2\} - 16T\mathcal{E}_2\{\tau^3\} + 8\mathcal{E}_2\{\tau^4\}) & \\ \quad + A^2\sigma_n^2(\frac{15}{4}T^2\mathcal{E}_2\{1\} - 12T\mathcal{E}_2\{\tau\} + 12\mathcal{E}_2\{\tau^2\}) + 3\sigma_n^4\mathcal{E}_2\{1\} & \frac{T}{4} \leq \tau < \frac{T}{2} \end{cases} \tag{D-7}$$

$$\mathcal{E}\{Q_k^4\} = \begin{cases} A^4(\frac{T^4}{32}\mathcal{E}_1\{1\} + 8\mathcal{E}_1\{\tau^4\}) + A^2\sigma_n^2(\frac{3}{4}T^2\mathcal{E}_1\{1\} + 12\mathcal{E}_1\{\tau^2\}) + 3\sigma_n^4\mathcal{E}_1\{1\} & 0 \leq \tau < \frac{T}{4} \\ (\frac{A^4T^4}{16} + \frac{3}{2}A^2T^2\sigma_n^2 + 3\sigma_n^4)\mathcal{E}_2\{1\} & \frac{T}{4} \leq \tau < \frac{T}{2} \end{cases} \tag{D-8}$$

Appendix E

Derivation of the Mean and Variance of the AVNOD

By following the same procedure as in Appendix B and by using

$$\mathcal{E}\{|I_k|\} = \begin{cases} \mathcal{E}_1\{|\frac{AT}{2} + N|\} & 0 \le \tau < \frac{T}{4} \\ \frac{1}{2}[\mathcal{E}_2\{|\frac{AT}{2} + N|\} + \mathcal{E}_2\{|AT - 2A\tau + N|\}] & \frac{T}{4} \le \tau < \frac{T}{2} \end{cases} \tag{E-1}$$

$$\mathcal{E}\{|Q_k|\} = \begin{cases} \frac{1}{2}[\mathcal{E}_1\{|\frac{AT}{2} + N|\} + \mathcal{E}_1\{|2A\tau + N|\}] & 0 \le \tau < \frac{T}{4} \\ \mathcal{E}_2\{|\frac{AT}{2} + N|\} & \frac{T}{4} \le \tau < \frac{T}{2} \end{cases} \tag{E-2}$$

and

$$\mathrm{Var}(|I_k| - |Q_k|) = \begin{cases} \frac{3A^2T^2}{8}\mathcal{E}_1\{1\} + 2A^2\mathcal{E}_1\{\tau^2\} + 2\sigma_n^2\mathcal{E}_1\{1\} \\ \quad -\frac{5}{4}\mathcal{E}_1^2\{|\frac{AT}{2} + N|\} - \frac{1}{4}\mathcal{E}_1^2\{|2A\tau + N|\} \\ \quad -\frac{1}{2}\mathcal{E}\{|\frac{AT}{2} + N|\}\mathcal{E}_1\{|2A\tau + N|\} & 0 \le \tau < \frac{T}{4} \\ \frac{7A^2T^2}{8}\mathcal{E}_2\{1\} - 2A^2T\mathcal{E}_2\{\tau\} + 2A^2\mathcal{E}_2\{\tau^2\} + 2\sigma_n^2\mathcal{E}_2\{1\} \\ \quad -\frac{5}{4}\mathcal{E}_2^2\{|\frac{AT}{2} + N|\} - \frac{1}{4}\mathcal{E}_2^2\{|AT - 2A\tau + N|\} \\ \quad -\frac{1}{2}\mathcal{E}\{|\frac{AT}{2} + N|\}\mathcal{E}_2\{|AT - 2A\tau + N|\} & \frac{T}{4} \le \tau < \frac{T}{2} \end{cases} \tag{E-3}$$

one obtains Eqs. (40) through (45) after using the results of Appendix C and lengthy manipulations. The function Z in Eq. (45) is defined as

$$Z(\eta_s) \triangleq \mathcal{E}_1\{|(u + cn_1)(u + cn_2)|\} \tag{E-4}$$

where $c \triangleq 1/(2\sqrt{\eta_s})$, the n_i's are normal independent random variables with zero mean and unit variance, and u is a uniform random variable in the range (0, 1). In Z, the expectation with respect to u is over the range [0, 1/4] and the function is plotted in Fig. B-2 versus the symbol SNR (η_s).

Appendix F

Derivation of the Mean and Variance of the SPED

The samples I_k and Q_k are given by Eqs. (47) and (48). The output of the lock detector is $x_k = I_k Q_k$. It is straightforward to show that

$$\mathcal{E}\{X_k\} = \frac{A^2T^2}{4} - \frac{A^2T}{2}\mathcal{E}\{\tau\} \tag{F-1}$$

and

$$\mathcal{E}\{X_k^2\} = A^4\left(\frac{T^4}{16} - \frac{T^3\mathcal{E}\{\tau\}}{4} + \frac{T^2\mathcal{E}\{\tau^2\}}{2}\right) + \sigma_n^4 + A^2\sigma_n^2\left(\frac{T^2}{2} - T\mathcal{E}\{\tau\} + 2\mathcal{E}\{\tau^2\}\right) \tag{F-2}$$

$$\mathrm{Cov}(X_k, X_{k+j}) = \begin{cases} \frac{A^4T^2}{4}\mathrm{Var}(\tau) & \tau \sim u(0, \frac{T}{2}) \text{ and } j \geq 1 \\ 0 & \tau = 0 \end{cases} \tag{F-3}$$

Equations (49) and (50) follow after letting $\tau = 0$ in Eqs. (F-1) through (F-3). Equations (51) and (52) follow by letting τ be uniform over $[0,\ T/2]$.